이학석사학위논문

Light-Induced pH-Responsive Degradation of Fumaramic Acid Derivatives

2015년 2월

서울대학교 대학원

화학부 생화학 전공

최 원 민 (Wonmin Choi)

Light-Induced pH-Responsive Degradation of Fumaramic Acid Derivatives

지도교수 이 연

이 논문을 이학석사학위논문으로 제출함

2015년 2월

서울대학교 대학원
화학부 생화학 전공
최 원 민 (Wonmin Choi)

최원민 (Wonmin Choi)의 석사학위논문을 인준함
2015년 2월

위 원 장 박 종상 (인)
부 위 원 장 이 연 (인)
위 원 김 성훈 (인)

Abstract

Light-Induced pH-Responsive Degradation of Fumaramic Acid Derivatives

최 원 민 **(Wonmin Choi)**
Department of Chemistry
College of Natural Sciences
Seoul National University

Fumaramic acid derivatives can be converted into their cis-isomer maleamic acid derivatives under UV illumination, and these maleamic acid derivatives show pH-responsive degradability at acidic pH only after the preceding photoisomerization. The rate of the tandem photoisomerization-degradation of fumaramic acid derivatives can be finely controlled by changing the substituents on the double bond. Photoisomerization-based unlocking of the pH-responsive degradability of fumaramic acid derivatives has strong potential for the development of multi-signal-responsive smart materials in biomedical applications.

Keyword: photoisomerization, pH-sensitivity, signal-responsiveness, tandem reaction, selectivity, photochemical reaction

Student number: 2013-20283

Contents

1. Introduction

Signal-responsive chemical moieties have been investigated for the development of smart materials. Chemical signals, including pH, [1] glutathione [2] and enzymes, [3] as well as physical signals, including temperature [4] and light, [5] have been used as triggers to induce characteristic changes in smart materials. Furthermore, dual-signal-responsive moieties were also developed to overcome the limited selectivity and sensitivity of single-signal responsiveness, as well as for use in more complex applications. [6] Dual-signal-responsive moieties, however, are mostly parallel combinations of two single-signal-responsive moieties. For example, a polymer with both a pH-sensitive imine linker and a light-sensitive o-nitrobenzyl succinate (NBS) linker has been considered a dual-signal-responsive polymer. [7] Examples of a unique single chemical moiety that can respond to both signals are difficult to find.

Maleic acid derivatives might be candidates for such chemical moieties because they respond to both signals. Light-induced cis-trans isomerization between maleic acid and fumaric acid has been well-known for decades, [8] and interconversion between maleamide and fumaramide was used to control the geometric change in the molecules. [9] Meanwhile, maleamic acid (or maleic acid amide) derivatives showed rapid degradability at weakly acidic pH due to the cis-conformation between the amide and carboxylate groups, expanding their applicability in drug delivery. [10] The responding pH values can be finely tuned by changing the substituents on the cis-double bonds. [11] Considering the structural similarity of maleic acid, maleamide, and maleamic acid, I expected that the pH-responsive de-

gradability of maleamic acid derivatives would be controllable by photoisomerization of the double bonds, although no reports have described the photoisomerization of maleamic acid derivatives.

In this communication, I intended to generate maleamic acid derivatives from the corresponding trans-isomer, fumaramic acid derivatives through photoisomerization (Figure 1). The initial fumaramic acid derivatives do not possess pH-responsive degradability because the cis-attack of the carboxylate group on the amide group is essential for their degradability at weakly acidic pH. [12] If the fumaramic acid derivatives can be converted to maleamic acid derivatives by exposure to light, the pH-responsiveness can be unlocked to degrade the amide bonds. Moreover, the pH that the derivatives respond to can also be delicately controlled by changing the substituents of the initial trans-double bonds of the fumaramic acid derivatives. Because the physiological pH differences are not very extreme, with few exceptions, [13] the photo-induced unlocking of degradability under specific pH conditions might have high applicability in the biomedical field.

2. Materials and methods

2.1. Materials

Mono-ethyl fumarate, glyoxylic acid monohydrate, n-butylamine, methyl 2-bromopropionate, triphenylphosphine, phosphorus tribromide and 4-(dimethylamino)pyridine (4-DMAP) were purchased from Sigma-Aldrich (St.Louis,MO,USA).

Ethyl-mandelate, 1-(3-dimethylaminopropyl)-3-ethylcarbodiimide hydrochloride (EDCI-HCl), and N,N-diisopropyl-ethylamine (DIPEA) were purchased from TCI (Japan). Magnesium sulfate ($MgSO_4$), sodium chloride (NaCl), sodium hydroxide (NaOH), sodium bicarbonate ($NaHCO_3$), sodium phosphate monobasic (NaH_2PO_4), acetonitrile(ACN), hexane, ethyl acetate (EA), ethanol (EtOH), dichloromethane (DCM), methanol (MeOH), hydrochloric acid (HCl), pyridine, and dimethyl sulfoxide (DMSO) were purchased from Daejung (South Korea). Anhydrous ACN, DCM, and DIPEA were obtained by distillation of the reagent-grade materials. Other reagents were used without further purification.

2.2. Syntheses of fumaramic acid derivatives

2.2.1. General procedure for synthesizing the fumaramic acid derivatives

N-butyl amine (0.9 eq) and 4-DMAP (1.0 eq) were added to a stirred solution of fumaric acid ester derivatives (1.0 eq) in anhydrous

DCM. After the reaction mixture was cooled in an ice bath. EDCI-HCl (1.0 eq) was added. After stirring for 24 h, the reaction mixture was washed with a saturated solution of citric acid and water. The N-butyl fumaramic ester derivative was obtained as a white solid after evaporation of the solvent.

The N-butyl fumaramic ester derivative (1.0 eq) was subsequently dissolved in EtOH, and NaOH (3.0 eq) in water was added. After stirring for 3 h, the solvent was evaporated, and the pH was adjusted to 1-2 with 0.5 M HCl (aq). The combined water phase was extracted with EA, and the organic layer was dried over $MgSO_4$. The N-butyl fumaramic acid derivatives were obtained as white solids after evaporation of the solvent.

2.2.2 N-butyl 3-methyl fumaramic acid (2)

Methyl 2-bromopropionate (1.0 eq) was dissolved in anhydrous ACN, and triphenylphosphine (0.9 eq) was added under a nitrogen atmosphere. After stirring the mixture at 65°C for 9 h, it was placed at 0°C, and glyoxylic acid monohydrate (0.7 eq) and anhydrous DIPEA (0.7 eq) were added. After stirring for 2 h, the temperature was elevated to ambient temperature, and after further stirring for 24 h, the mixture was concentrated using a rotary evaporator. The phases of the crude product were then separated with EA and a saturated $NaHCO_3$ solution. The aqueous layer was collected and adjusted to pH 1-2 with concentrated HCl at 0°C. The acidified solution was extracted with EA, and the EA layer was dried over $MgSO_4$ and concentrated to yield pure 3-methyl fumaric acid ester (yield: 82%). The subsequent steps followed the general procedure.

2.2.3 N-butyl 3-phenyl fumaramic acid (3)

Ethyl mandelate (1.0 eq) was dissolved in DCM at 0°C under inert conditions; phosphorus tribromide (0.7 eq) was then added to this solution, and the solution was stirred for 1 h and then quenched with distilled water. The phases of the mixture were then separated with EA and brine, and the organic layer was collected and dried over $MgSO_4$. The crude product was purified by silica gel chromatography and eluted with EA/hexane to yield pure ethyla-bromophenyl acetate as a colorless oil (yield: 89%).

Ethyl α-bromophenyl acetate (1.0 eq) was dissolved in ACN, and triphenylphosphine (0.9 eq) was added under a nitrogen atmosphere. After stirring the mixture for 9 h at 65°C, the mixture was placed at 0°C, and glyoxylic acid monohydrate (0.7 eq) and anhydrous DIPEA (0.7 eq) were added. After stirring for 2 h, the temperature was elevated to ambient temperature, and after further stirring for 24 h, the mixture was concentrated using a rotary evaporator. The phases of the crude product were then separated with EA and saturated $NaHCO_3$ solution, and the aqueous layer was collected and adjusted to pH 1-2 with concentrated HCl at 0°C. The acidified solution was extracted with EA, and the EA layer was dried over $MgSO_4$ and concentrated to yield pure 3-phenyl fumaric acid ester (yield: 65%). The subsequent steps followed the general procedure.

2.3. Changes in ^{1}H-NMR spectra due to photoisomerization

Each sample was prepared at a concentration of 1 mg/mL. The NMR spectrum was recorded using a Bruker Avance DPX-300 (Germany) or a Varian AS-500 (USA) spectrometer.

2.4. Changes in ^{1}H-NMR spectra due to photoisomerization

Each compound (1-3) was dissolved in a co-solvent (D_2O-based potassium phosphate buffer (50mM; pH7.4):CD_3OD=2:1), the solution was irradiated with UV light (365nm) at 37°C, and the ^{1}H-NMR spectra were observed. A LICHTZEN UV Lamp (INNO-CURE150, South Korea) equipped with a liquid light guide (LS15-1000, South Korea) and Edmund optical filters (Hard-coated od4 25-nm bandpass filters, NJ, USA) were used for the photoisomerization measurement. The UV intensity at 365nm were measured as 15mW/cm^2 for irradiation between the sample and the UV lamp, verified by a power meter (NOVAP/Z1Z01500,OPHIR,USA) equipped with a detector (30A-V1, OPHIR, USA).

2.5. Changes in ^{1}H-NMR spectra due to degradation

Each compound (4-6) was dissolved in a co-solvent (D_2O-based potassium phosphate buffer (50mM):CD_3OD=2:1), and the pH was adjusted with DCl. After incubation at 37°C for 12h, the ^{1}H-NMR spectra were observed.

2.6. Measurement of photoisomerization-degradation kinetics

Each fumaric acid derivative (1-3) (0.5 mM) was dissolved in a co-solvent (sodium phosphate buffer (50 mM; pH 4.5, pH 5.5, pH 7.4) containing 150 mM NaCl:MeOH = 2:1). The solution was then incubated with UV illumination and stirring at 37°C.

At various time points, a sample was collected and diluted four times with a phosphate buffer (50 mM, pH 9.0) containing 150 mM NaCl, and the extent of photoisomerization-degradation of the fumaramic acid derivatives was measured using HPLC. For the HPLC-based measurement, a YOUNGLIN HPLC (Acme 9000 HPLC, South Korea) equipped with a UV detector and a reverse-phase column (Agilent Eclipse XDB-C18 4.6 × 150 mm, 5 μm) was used. A mixture (1:9 v/v) of methanol:phosphate buffer (50 mM, pH 9.0) was used as the eluent, and the flow rate was set at 0.5 mL/min. Elution of the sample was detected by UV absorbance at 220 and 254 nm, and the extent of photoisomerization/degradation of each sample was measured three times at each time point.

3. Results & Discussion

To confirm my concept, I synthesized three model fumaramic acid derivatives: N-butyl fumaramic acid (1), N-butyl mesaconamic acid (N-butyl 3-methyl fumaramic acid) (2), and N-butyl 3-phenyl fumaramic acid (3) (Figure 1). All model compounds were synthesized from the corresponding fumaric acid monoester derivatives. Mesaconic acid monoester and 2-phenyl fumaric acid monoester were synthesized by the Wittig reaction, and the amide bond between the monoester and n-butylamine was formed by the carbodiimide reaction. Finally, the ester was hydrolyzed to produce the model compounds 1-3. The detailed synthetic procedure is described in the Figure 4.

Although numerous reports have described fumaric acid-maleic acid (diacid) and fumaramide-maleamide (diamide) isomerization due to exposure to light, the photoisomerization of amic acid, the intermediate compound between the diacid and the diamide, has never been reported to my knowledge. To photoisomerize amic acid, I used UV irradiation at a maximum wavelength of 365 nm from the high-pressure mercury lamp (15mW/cm^2 for irradiation) that was used in the isomerization of the diacid or diamide. [9] Figure 2a shows the change in the ^{1}H-NMR spectrum of 1 after irradiation. Clearly, compound 1 was converted to its corresponding cis-isomer (4) by UV irradiation. I also examined the possibility that the reverse photoisomerization reaction, from the cis-isomer to the trans-isomer, may occur. When compound 4 was irradiated by UV at the same wavelength, no peak corresponding to compound 1 was observed (data not shown). Unlike the photoisomerization of diacids [8] or diamides, [9] which reaches an equilibrium photostationary state between two

isomers, the reaction of fumaramic acid seems to be an irreversible, one-way reaction at this wavelength.

In the absence of UV irradiation, compound 1, the trans isomer, showed no pH-responsive degradability (data not shown). By contrast, the trans carboxylate group of compound 1 was converted to a cis carboxylate group by irradiation, and this group was positioned such that it was aimed at the carbonyl group of the amide and therefore primed for intramolecular nucleophilic attack. The unlocked pH-responsive degradability of the amic acid could be observed by ^{1}H-NMR (Figure2b). Although compound4 was stable at neutral pH, it was degraded to release free n-butylamine below pH 3.0. The kinetics of the pH-responsive degradation of compound 4 was measured in detail in previous report. [11]

Because the kinetics of photoisomerization and degradation was difficult to measure by ^{1}H-NMR due to the marginal solubility of compounds 1-9 in water-based buffers, the kinetics was measured by HPLC in more dilute solutions with the addition of methanol as a co-solvent. The tandem photoisomerization-degradation reaction can be expressed as follows:

$$Fum \overset{k_1}{\rightarrow} Mal \overset{k_2}{\rightarrow} Deg$$

In this equation, k_1 and k_2 are the reaction constants of photoisomerization and degradation, respectively, Fum is the fumaramic acid derivative (1-3), Mal is the maleamic acid derivative (4-6), and Deg is the anhydride degradation product (7-9).

The kinetics of the tandem reaction (photoisomerization-degradation) of compound 1-3 is shown in Figure 3 and Figure 8-11. As the amount of trans-isomer (compound 1-3) decreased after UV irradi-

ation, the amount of cis-isomer (compound 4-6) increased. Meanwhile, the amount of the degradation product (compound 7-9) slowly increased. If I assume that both tandem reactions follow the first-order kinetics of the reactants, the rate constants, k_1 and k_2, can be calculated from the observed data by regression. The calculated rate constants are summarized in Table1.

The photoisomerization rate of compound 1 was pH-dependent (Figure 9), and the initial isomerization rate constant at pH 3.0 (k_1=34.7×10^{-3} min^{-1}) was more than four times higher than that at pH7.4 (k_1=8.41×10^{-3} min^{-1}). I hypothesized that the isomerization rate increased as the pH decreased because the protonated form absorbed UV light more efficiently than the deprotonated form. This hypothesis was supported by the observation that the extinction coefficient of compound 1 at 365 nm and pH 3.0 (ε_{365}=62.6 $M^{-1}\cdot cm^{-1}$) was 3.7 times higher than that at pH 7.4 (ε_{365}=17.0 $M^{-1}\cdot cm^{-1}$) (Table1).

Although the photo-induced unlocking of the pH-responsive degradability of compound 1 was confirmed (Figure 2), the responding pH (3.0) is too extreme to have a wide range of applications in the biomedical field. Above pH 4.5, compound 1 only showed photoisomerization without successive degradation (Figure 3a, Figure 10a, 11a). Therefore, I further analyzed the tandem photoisomerization-degradation of compounds 2 and 3 with 3-methyl and 3-phenyl substituents, respectively. Because the maleamic acid derivatives with bulkier substituents exhibited degradability at higher pH compared to the non-substituted derivatives, [11] I expected that the photoisomerized cis isomers, compounds 5 and 6, would show pH-responsive degradability at mild acidic pH. Figures 3b and 3c show the

kinetics of the tandem reactions of compounds 2 and 3, respectively, at pH 4.5. Compounds 2 and 3 exhibited accelerated photoisomerization as well as degradation at pH 4.5 compared to compound 1. The higher extinction coefficients of compounds 2 and 3 compared to that of compound 1 partially explained the higher photoisomerization rates. Compound 2 showed a degradation rate of k_2 of 2.76×10^{-3} min^{-1} at pH 4.5 (Table 1) and did not show any degradation above pH 5.5 (Figure 10b, 11b); however, the tandem reaction of compound 3 with a bulkier phenyl substituent exhibited a much faster rate of degradation at pH 4.5 ($k_2=32.1\times10^{-3}$ min^{-1}). Slower ($k_2=5.13\times10^{-3}$ min^{-1}) or no degradation was observed at pH 5.5 and pH 7.4, respectively (Figure 10c, 11c). Therefore, when an amine-containing drug other than n-butylamine is conjugated to a drug carrier through a fumaric acid derivative linker with a bulkier substituent, the drug molecules can be released at mild acidic pH only after photo-induced unlocking of the fumaramic acid derivatives.

4. Conclusion

The pH signal is a delicate internal biochemical indicator in the body. Under abnormal conditions, such as cancer, inflammation, or abscesses, the pH value of the physiological fluid is lowered to 5.0-6.5 from the normal pH value of 7.4. [14] Meanwhile, light is usually used as an external signal to trigger a photochemical reaction at a target site owing to the focusing ability of the illumination. [15] In this research, I showed the unique dual pH- and light-responsiveness of fumaramic acid derivatives. The pH-responsive degradability of fumaramic acid derivatives can be unlocked only after they isomerize into maleamic acid derivatives in response to illumination, and the advantages of pH- and light-signal-responsiveness can be intrinsically combined in the structure of fumaramic acid derivatives. Furthermore, bulkier and more light-absorbing substituents, such as the 3-phenyl group, can accelerate both the photoisomerization rate and pH-responsive degradability. In future research, the responding pH and wavelength should be tuned to the range of pH 5~6 and near infrared (NIR), respectively, by changing the structure of the substituents to allow wider applicability in biomedical fields. [11, 16] Of course, on-site UV generation technique by NIR irradiation based on upconverting nanoparticles can also be used for a target-specific unlocking of pH-responsive degradability of fumaramic acid derivatives. [17]

5. References

[1] a) J. C. Yu, Y. L. Chen, Y. Q. Zhang, X. K. Yao, C. G. Qian, J. Huang, S. Zhu, X. Q. Jiang, Q. D. Shen, Z. Gu, Chem. Commun. 2014, 50, 4699-4702; b) N. S. Lee, Y. Li, C. M. Ruda, K. L. Wooley, Chem. Commun. 2008, 5339-5341.

[2] a) M. Zhao, A. Biswas, B. Hu, K. I. Joo, P. Wang, Z. Gu, Y. Tang, Biomaterials 2011, 32, 5223-5230; b) Y. Lee, H. Mo, H. Koo, J.-Y. Park, M. Y. Cho, G.-w. Jin, J.-S. Park, Bioconjugate Chem. 2006, 18, 13-18.

[3] A. Biswas, K.-I. Joo, J. Liu, M. Zhao, G. Fan, P. Wang, Z. Gu, Y. Tang, ACS Nano 2011, 5, 1385-1394.

[4] Y. Li, B. S. Lokitz, C. L. McCormick, Angew. Chem. Int. Ed. 2006, 45, 5792-5795.

[5] C. de Gracia Lux, A. Almutairi, ACS Macro Lett. 2013, 2, 432-435.

[6] a) J. H. Kim, E. Lee, J. S. Park, K. Kataoka, W. D. Jang, Chem. Commun. 2012, 48, 3662-3664; b) X. Tian, K.-H. Baek, I. Shin, Chem. Sci. 2013, 4, 947.

[7] L. Meng, W. Huang, D. Wang, X. Huang, X. Zhu, D. Yan, Biomacromolecules 2013, 14, 2601-2610.

[8] R. Fausto, E. M. S. Maçôas, J. Mol. Struct. 2001, 563–564, 27-40.

[9] P. Altoè, N. Haraszkiewicz, F. G. Gatti, P. G. Wiering, C. Frochot, A. M. Brouwer, G. Balkowski, D. Shaw, S. Woutersen, W. J. Buma, F. Zerbetto, G. Orlandi, D. A. Leigh, M. Garavelli, J. Am. Chem. Soc. 2008, 131, 104-117.

[10] a) S. Kang, E. Park, Y. Kim, S. Lee, J. Kwon, H. Cho, Y. Lee, J. Drug Targeting. 2014, 22, 658-668; b) Y. Lee, T. Ishii, H. Cabral, H. J. Kim, J. H. Seo, N. Nishiyama, H. Oshima, K. Osada, K.

Kataoka, Angew. Chem. Int. Ed. 2009, 48, 5309-5312.

[11] S. Kang, Y. Kim, Y. Song, J. U. Choi, E. Park, W. Choi, J. Park, Y. Lee, Bioorg. Med. Chem. Lett. 2014, 24, 2364-2367.

[12] a) A. J. Kirby, P. W. Lancaster, J. Chem. Soc., Perkin Trans. 2 1972, 1206-1214; b) A. J. Kirby, R. S. McDonald, C. R. Smith, J. Chem. Soc., Perkin Trans. 2 1974, 1495-1504.

[13] I. Mellman, R. Fuchs, A. Helenius, Annu. Rev. Biochem. 1986, 55, 663-700.

[14] W. Gao, J. M. Chan, O. C. Farokhzad, Mol. Pharmaceutics. 2010, 7, 1913-1920.

[15] M. Bostad, M. Kausberg, A. Weyergang, C. E. Olsen, K. Berg, A. Hogset, P. K. Selbo, Mol. Pharmaceutics. 2014, 11, 2764-2776.

[16] A. A. Beharry, O. Sadovski, G. A. Woolley, J. Am. Chem. Soc. 2011, 133, 19684-19687.

[17] J. Liu, W. Bu, L. Pan, J. Shi, Angew. Chem. Int. Ed. 2013, 52, 4375-4379.

6. Figures & Table

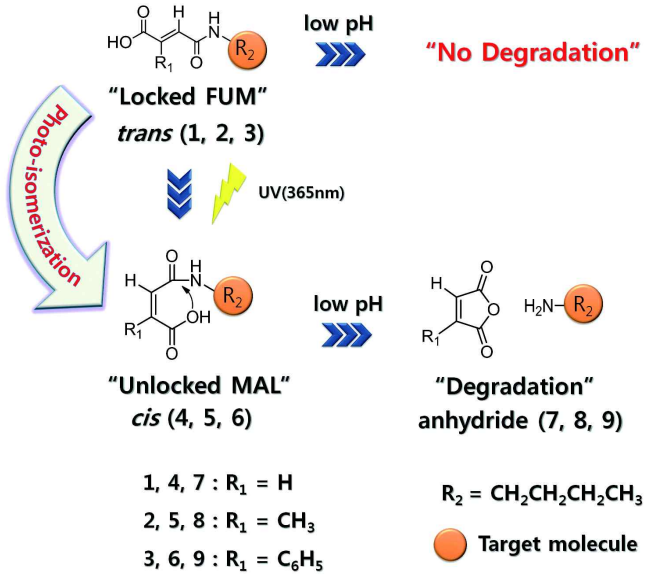

Fig 1. General scheme of the pH-responsive degradation of fumaramic acid derivatives unlocked by photoisomerization.

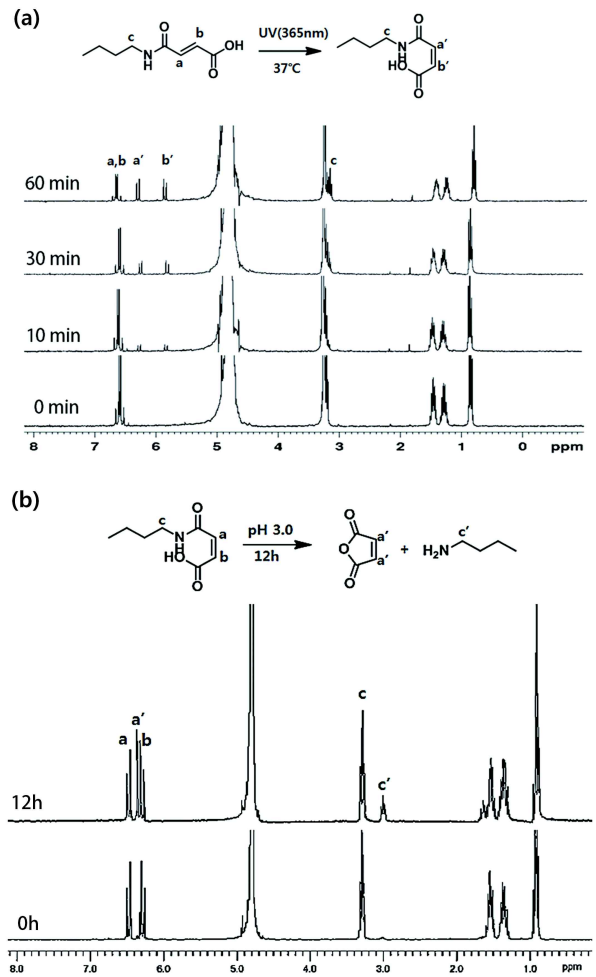

Fig 2. ^{1}H NMR spectra of (a) compound 1 during UV irradiation (pH 7.4) and (b) compound 4 during incubation at pH 3.0.

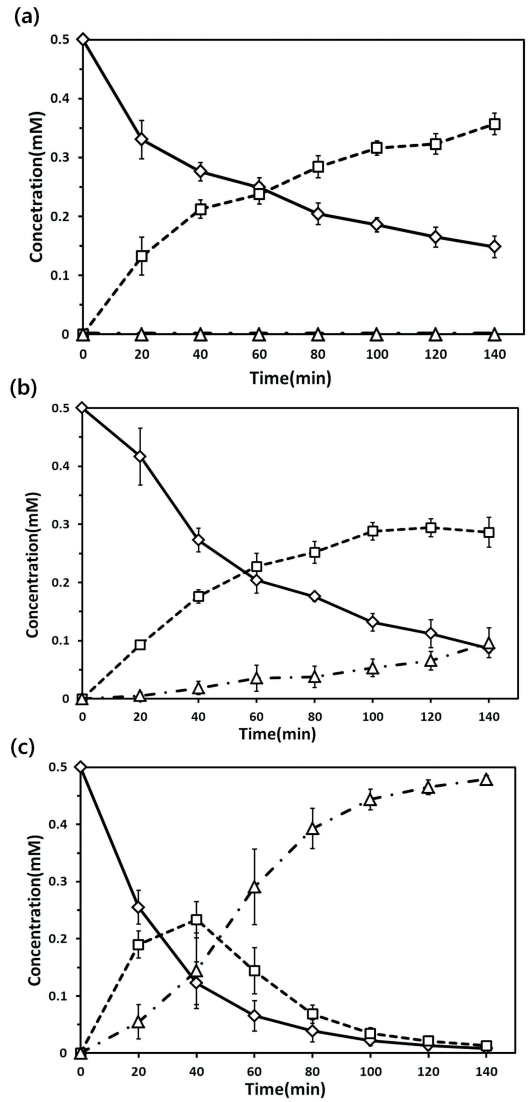

Fig 3. Reaction kinetics of the tandem photo-isomerization-degradation of (a) compound 1, (b) compound 2, and (c) compound 3 at pH 4.5 (Fum compounds (1-3) (◇); Mal compounds (4-6) (□); Deg compounds (7-9) (△)) Error bars represent the standard deviation (n = 3).

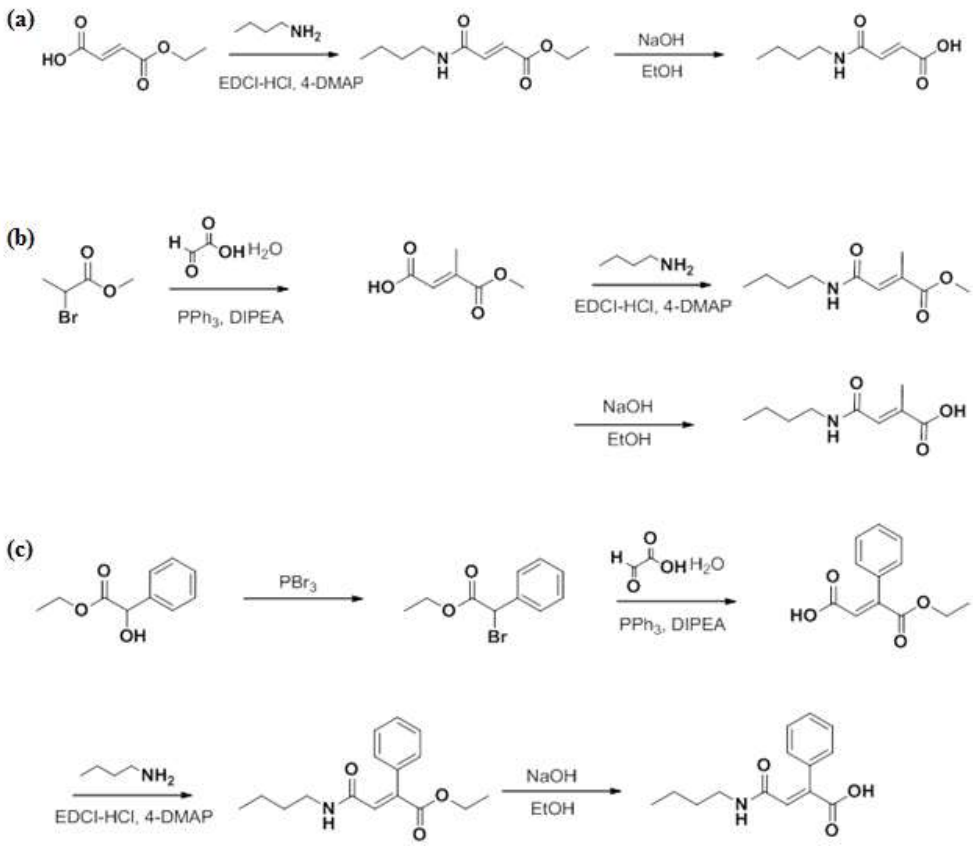

Fig 4. Synthetic scheme of (a) *N*-butyl fumaramic acid, (b) *N*-butyl 3-methyl fumaramic acid, (c) *N*-butyl 3-phenyl fumaramic acid.

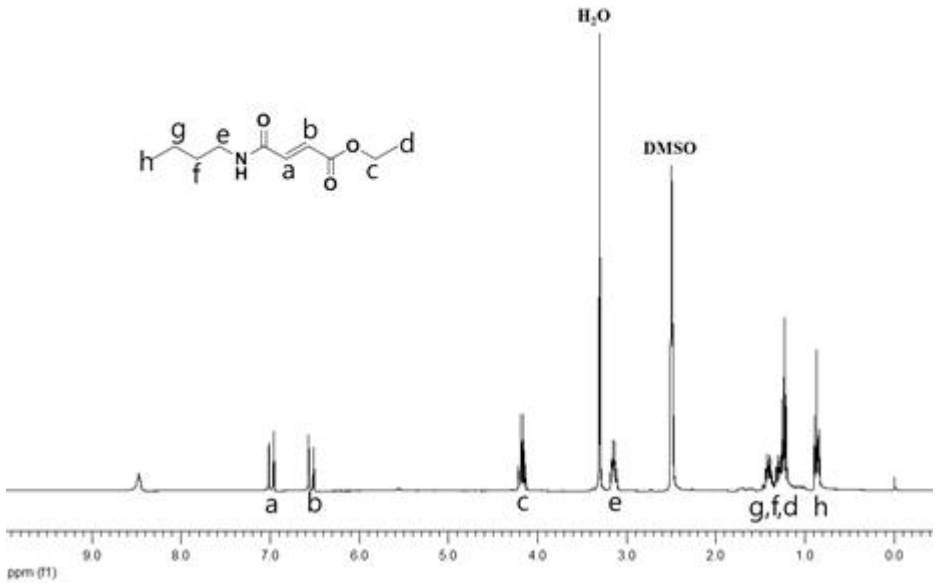

Fig 5-a). ^{1}H NMR spectra of *N*-butyl fumaramic ester in DMSO.

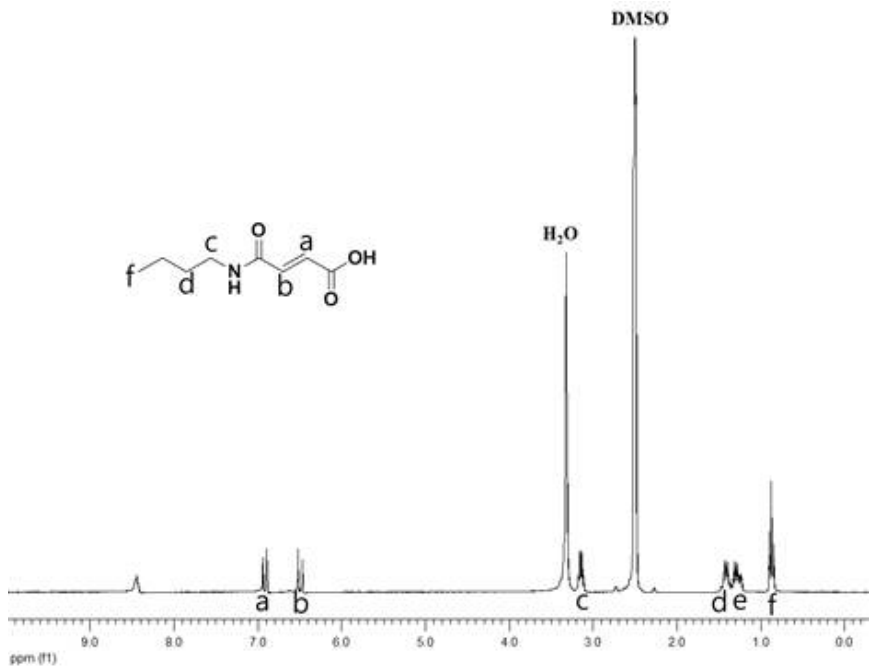

Fig 5-b). ^{1}H NMR spectra of *N*-butyl fumaramic acid in DMSO.

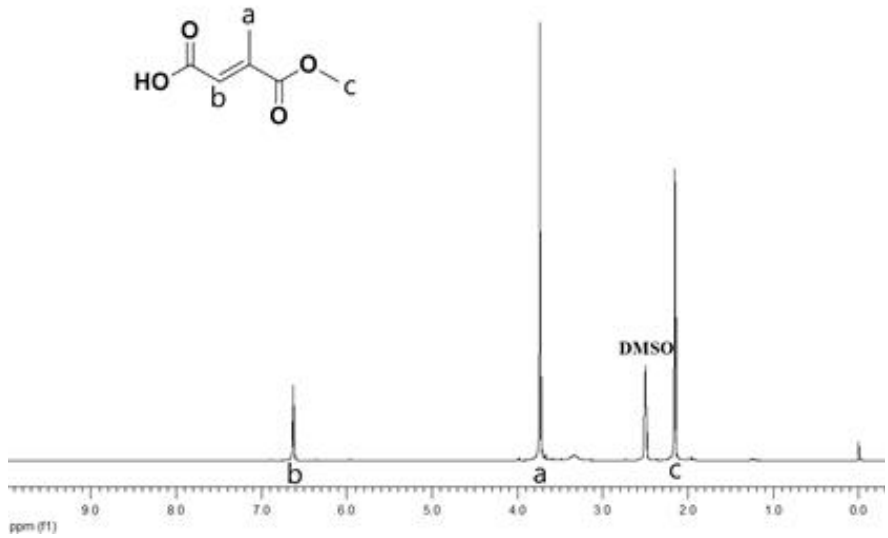

Fig 5-c). ^{1}H NMR spectra of 3-methyl fumaric acid ester in DMSO.

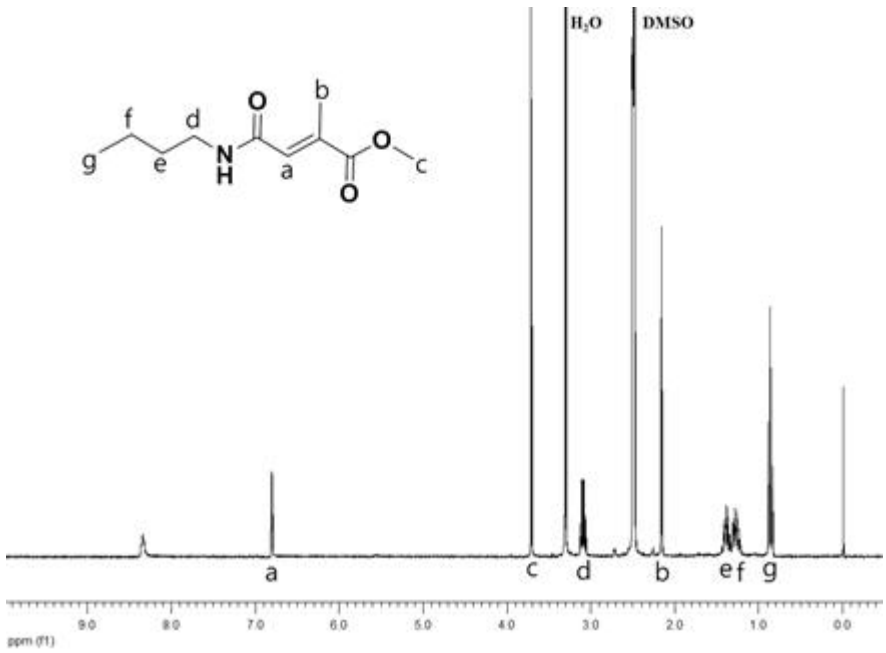

Fig 5-d). ^{1}H NMR spectra of *N*-butyl 3-mehtyl fumaramic ester in DMSO.

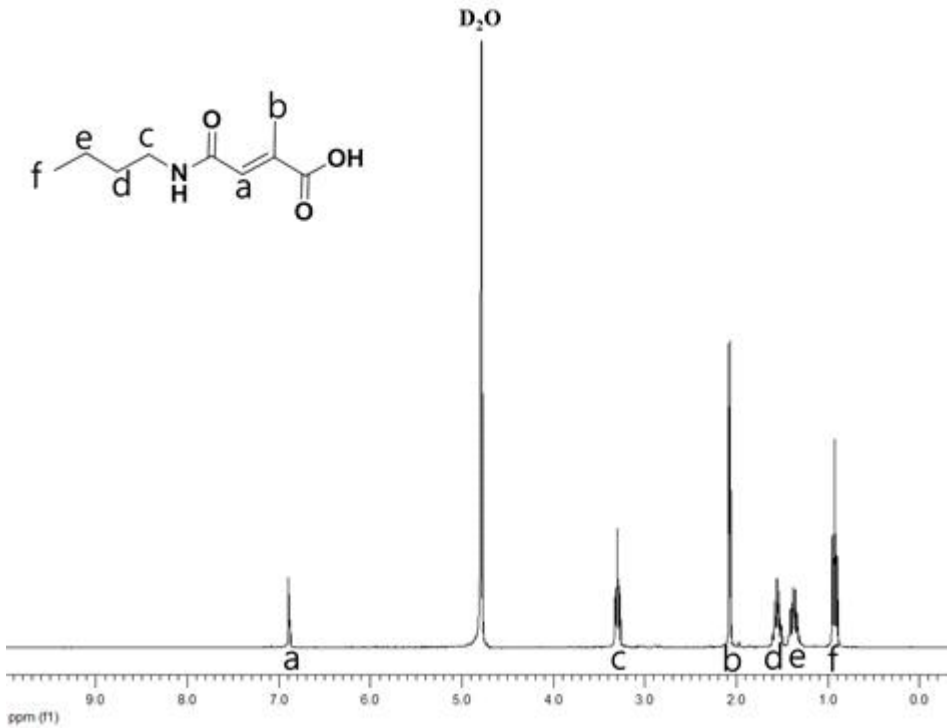

Fig 5-e). ^{1}H NMR spectra of *N*-butyl 3-mehtyl fumaramic acid in D_2O.

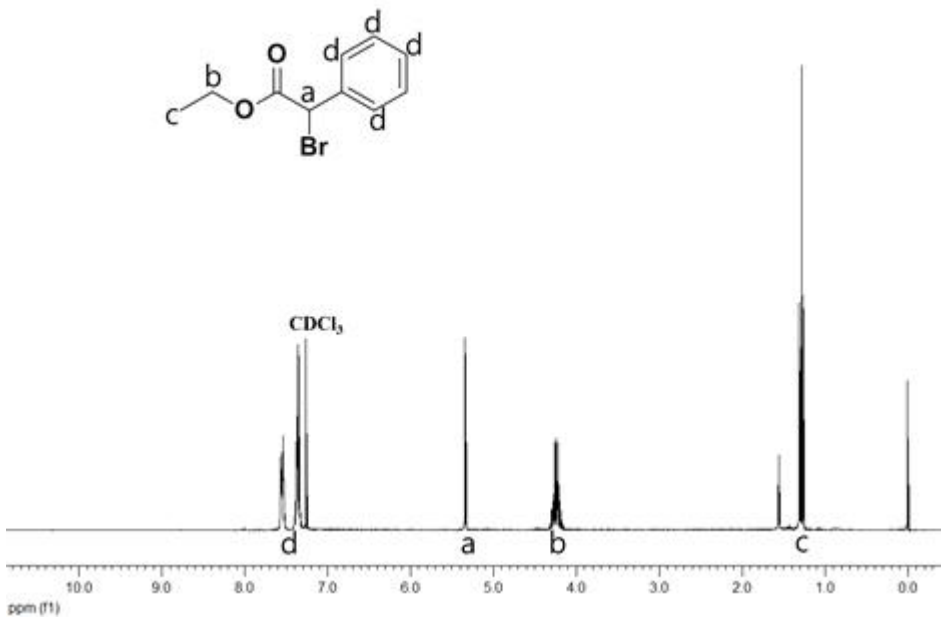

Fig 5-f). ^{1}H NMR spectra of Ethyl α-bromophenylacetate in $CDCl_3$.

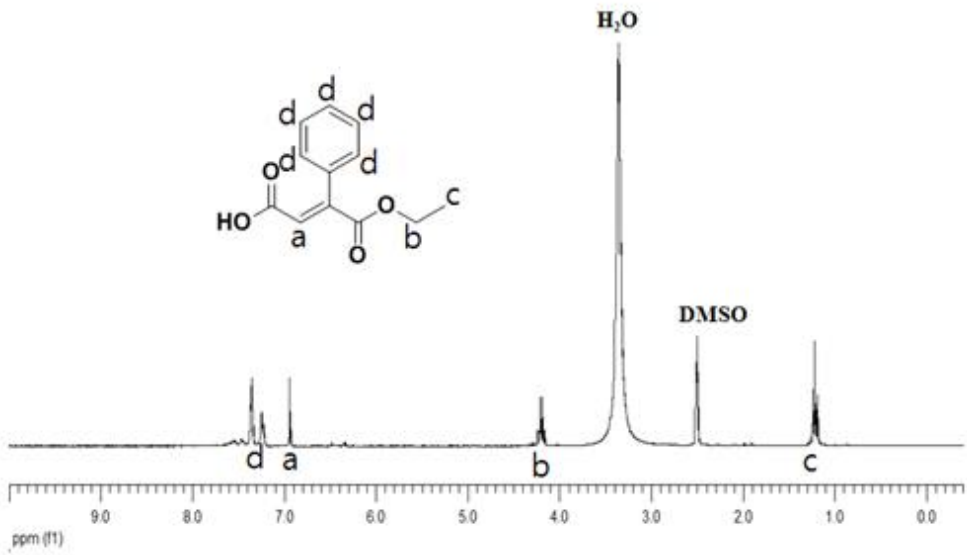

Fig 5-g). ^{1}H NMR spectra of 3-phenyl fumaric acid ester in DMSO.

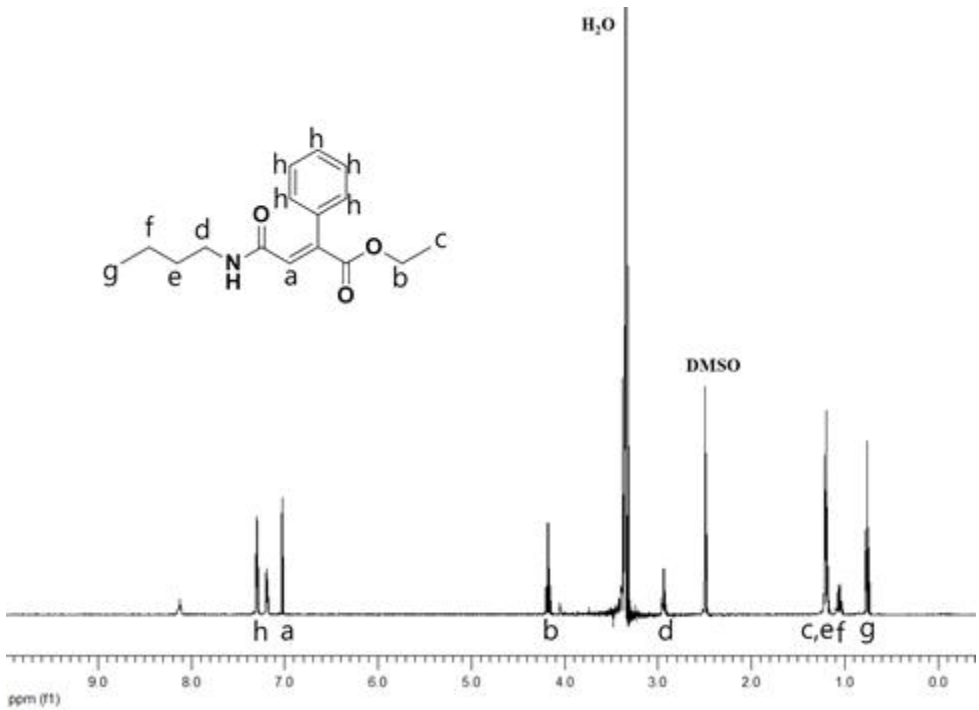

Fig 5-h). ^{1}H NMR spectra of 3-phenyl fumaramic ester in DMSO.

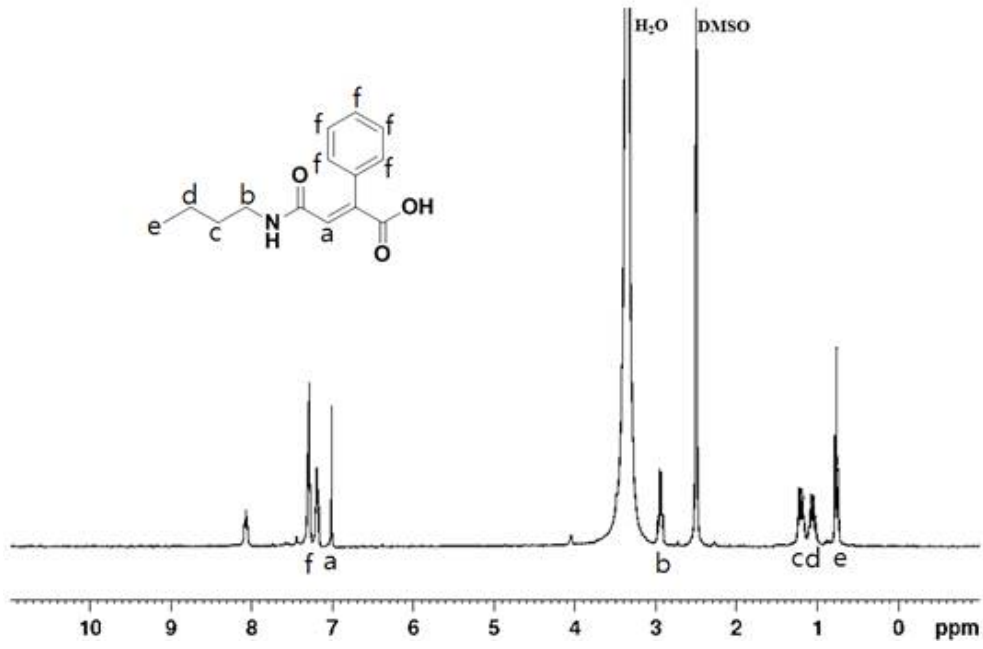

Fig 5-i). ^{1}H NMR spectra of *N*-butyl 3-phenyl fumaramic acid in DMSO.

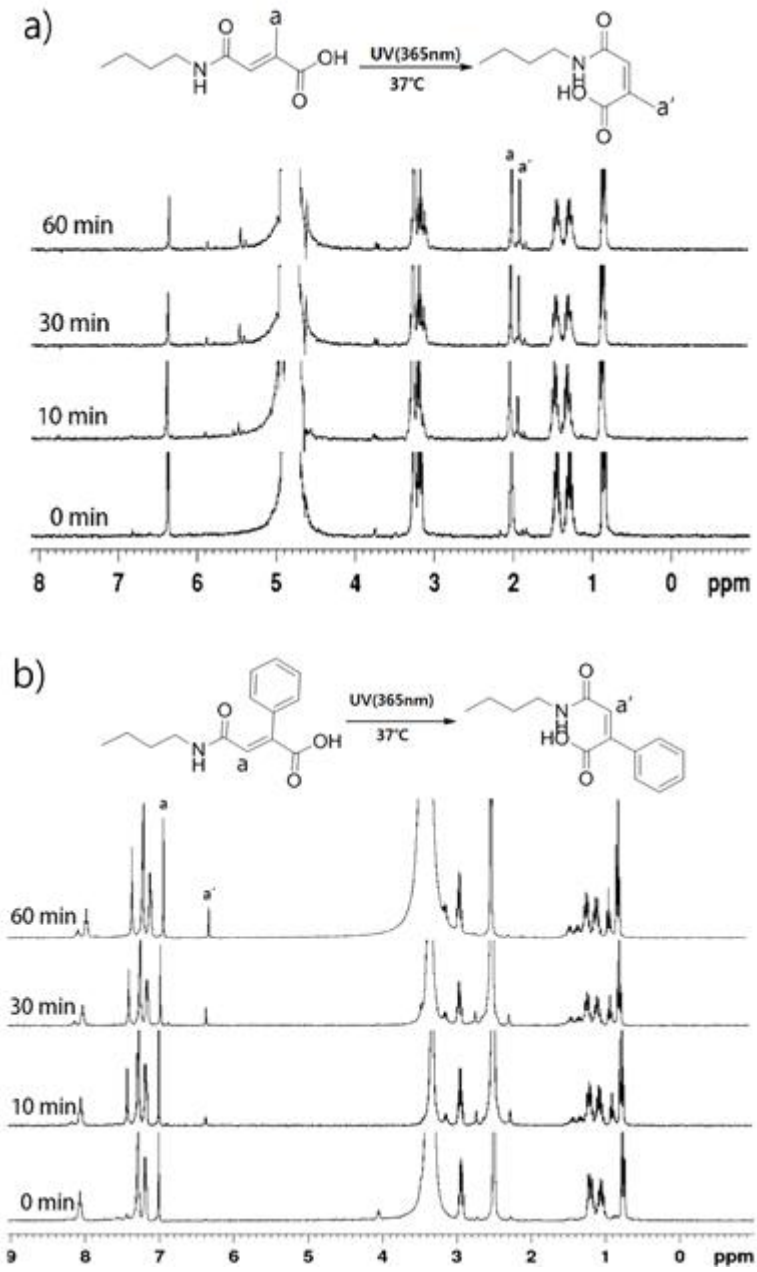

Fig 6. ^{1}H NMR spectra of a) *N*-butyl 3-methyl fumaramic acid (**2**) and b) *N*-butyl 3-phenyl fumaramic acid (**3**) during UV irradiation.

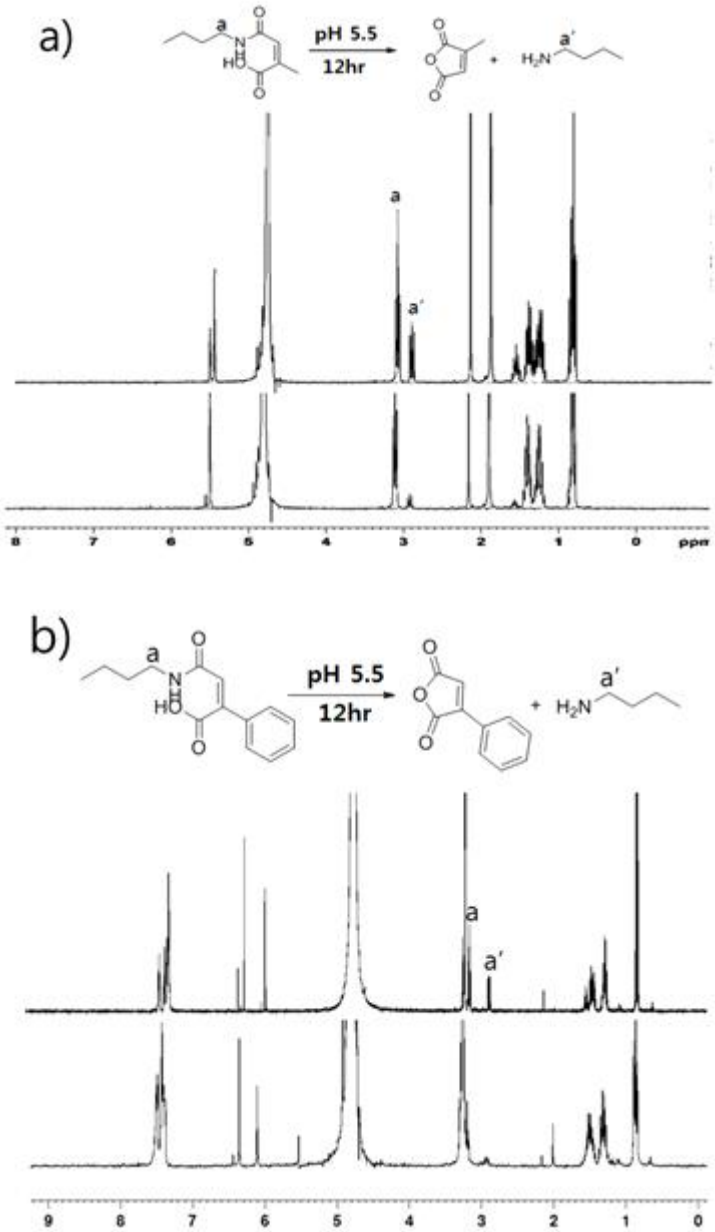

Fig 7. ^{1}H NMR spectra of a) compound **5** and b) compound **6** during incubation at pH 5.5.

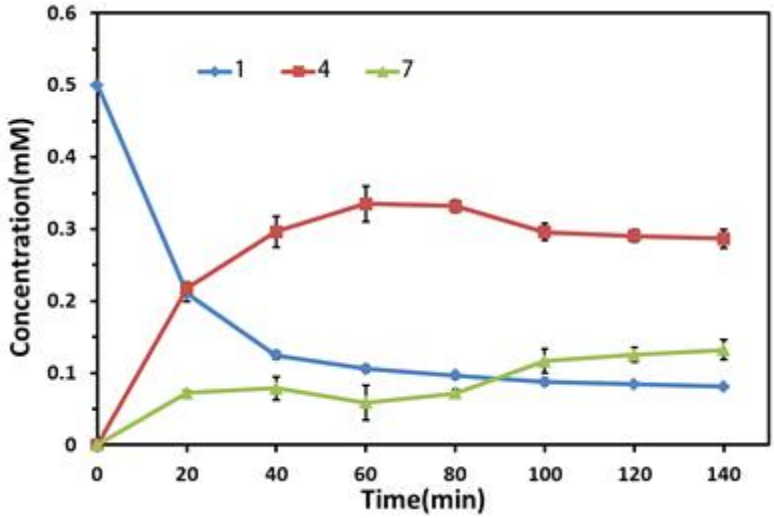

Fig 8. Reaction kinetics of the tandem photoisomerization-degradation of compound **1** at pH 3.0. Error bars represent the standard deviation (n = 3).

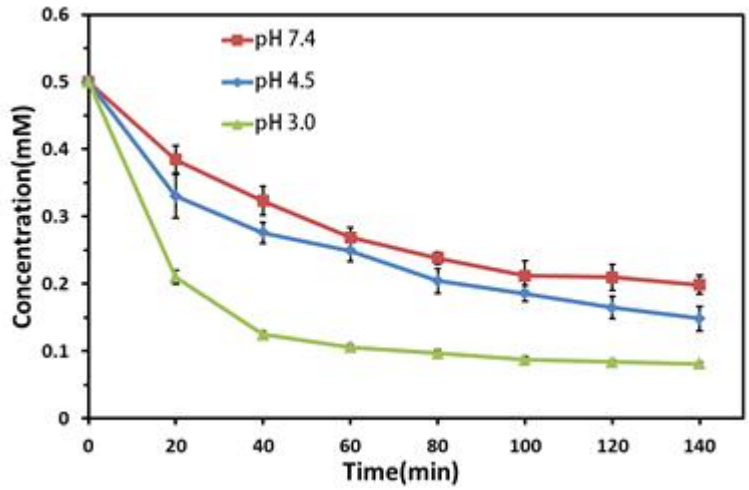

Fig 9. Comparison of photoisomerization rates of compound **1** at pH 3.0, 4.5, and 7.4. Error bars represent the standard deviation (n = 3).

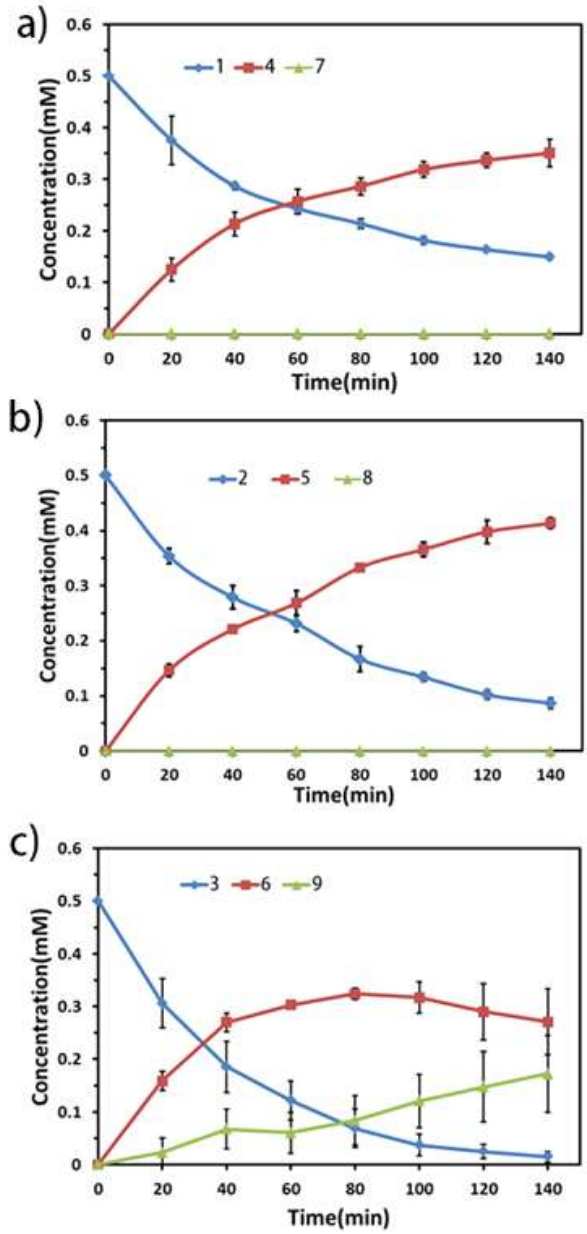

Fig 10. Reaction kinetics of the tandem photo-isomerization-degradation of compound a) **1**, b) **2**, and c) **3** at pH 5.5. Error bars represent the standard deviation (n = 3).

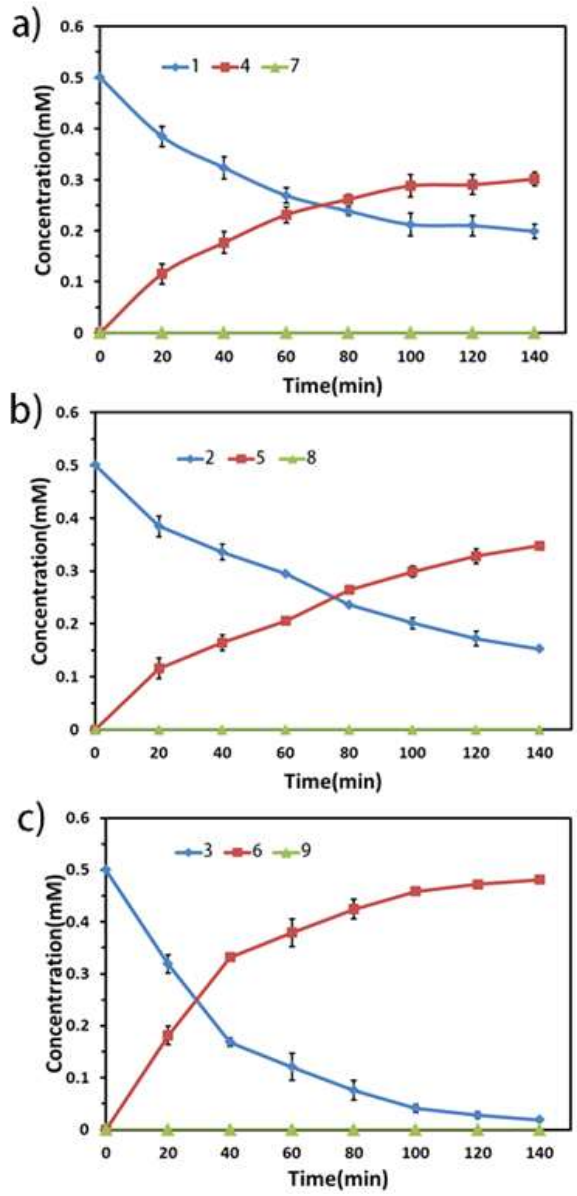

Fig 11. Reaction kinetics of the tandem photo-isomerization-degradation of compound a) **1**, b) **2**, and c) **3** at pH 7.4. Error bars represent the standard deviation (n = 3).

Compd	ε_{365} ($M^{-1}cm^{-1}$)[a]	k_1 ($\times 10^3 min^{-1}$)[b]	k_2 ($\times 10^3 min^{-1}$)[c]
1	17.0[d]/30.0[e]/37.8[f]/62.6[g]	8.41[d]/9.7[e]/10.9[f]/34.7[g]	6.29[g]
2	22.0[d]/38.9[e]/40.6[f]	8.91[d]/12.5[e]/13.3[f]	2.76[f]
3	43.9[d]/52.6[e]/59.2[f]	24.2[d]/26.8[e]/33.8[f]	5.13[e]/32.1[f]

[a]Molar absorptivity at 365nm. [b]Photoisomerization rate constant. [c]Degradation rate constant. Values at [d]pH7.4, [e]5.5, [f]4.5, and [g]3.0.

Table 1. Photophysical properties and kinetics of fumaramic acid derivatives.

국문 초록

Fumaramic 산 유도체는 UV light 조명 하에서 이성질체인 시스-이성질체 말레 산 유도체로 전환 될 수 있으며, 이들의 말레 산 유도체는 광-이성화 후 산성 pH 에서 pH 응답 분해성을 보여준다. 이러한 fumaramic 산 유도체의 광이성화 – pH 응답 분해성의 속도는 이중결합의 치환체를 변화시킴으로써 제어 될 수 있다. Fumaramic 산 유도체의 광-이성화 기반 pH 응답 분해성의 성질은 생물 의학 응용분야에서 다중 신호에 반응하는 스마트 재료의 개발을 위한 물질로써 강력한 잠재력을 가지고 있다.

주요어 : 광이성화, pH 응답 분해성, Tandem 반응, 선택성, 광화학 반응

학번 : 2013-20283